Supplemental Information
Computational Analysis of Particle Nucleation in Dilution Tunnels: Effects of Flow Configuration and Tunnel Geometry

Satbir Singh[a,*], Peter J. Adams[b], Ashwin Misquita[a], Kyung J. Lee[a], Eric M. Lipsky[c], Allen L. Robinson[a],

[a] *Mechanical Engineering, Carnegie Mellon University, Pittsburgh, PA, USA*
[b] *Civil and Environmental Engineering, Carnegie Mellon University, Pittsburgh, PA, USA*
[c] *Mechanical Engineering, Pennsylvania State Greater Allegheny, Pittsburgh, PA, USA*

S1. Numerical Formulation

S1.1. Mass and momentum transport

In large-eddy simulation (LES) of turbulent flows, large scale fluid motions are directly computed, while the influence of fluid motions of scales smaller than the computational cell size, is modeled using a subgrid-scale (SGS) model. The governing equations for LES are derived by the application of a low-pass spatial filter to the Navier-Stokes equations. The compressible flow LES equations available in CONVERGE code for conservation of mass and momentum become:

$$\begin{aligned} \frac{\partial \overline{\rho}}{\partial t} + \frac{\partial \overline{\rho}\tilde{u}_i}{\partial x_i} &= 0, \\ \frac{\partial \overline{\rho}\tilde{u}_i}{\partial t} + \frac{\partial \overline{\rho}\tilde{u}_i\tilde{u}_j}{\partial x_j} &= -\frac{\partial \overline{p}}{\partial x_i} + \frac{\partial}{\partial x_j}(\widetilde{\sigma}_{ij} - \tau_{ij}), \end{aligned} \tag{S1}$$

where $\widetilde{()}$ indicates Favre-filtered parameter and $\overline{()}$ indicates the grid-filtered parameter. $\widetilde{\sigma}_{ij}$ is the filtered viscous stress tensor and $\tau_{ij} = \overline{\rho}(\widetilde{u_i u_j} - \tilde{u}_i\tilde{u}_j)$ is the SGS stress tensor, which requires a model for closure. In this work,

*corresponding author: email - satbirs@andrew.cmu.edu

authors have implemented into CONVERGE an eddy-viscosity model based on gradient diffusion hypothesis to approximate the SGS stress as following:

$$\tau_{ij} - \frac{1}{3}\tau_{kk}\delta_{ij} = -2\nu_t \left(\widetilde{S}_{ij} - \frac{1}{3}\widetilde{S}_{kk}\delta_{ij} \right), \tag{S2}$$

where $\widetilde{S}_{ij} = \frac{1}{2}(\frac{\partial \tilde{u}_i}{\partial x_j} + \frac{\partial \tilde{u}_j}{\partial x_i})$ is the rate-of-strain tensor and ν_t is the eddy viscosity.

Eddy viscosity is calculated using following model proposed by Vreman (2004):

$$\nu_t = C_v \overline{\rho} \Pi, \tag{S3}$$

where

$$\begin{aligned}
\Pi &= \sqrt{\frac{B_\beta}{\widetilde{\alpha}_{kl}\widetilde{\alpha}_{kl}}}, \\
B_\beta &= \beta_{11}\beta_{22} - \beta_{12}\beta_{12} + \beta_{11}\beta_{33} - \beta_{13}\beta_{13} + \beta_{22}\beta_{33} - \beta_{23}\beta_{23}, \\
\beta_{ij} &= \sum_{m=1}^{3} \overline{\Delta}_m^2 \widetilde{\alpha}_{mi}\widetilde{\alpha}_{mj}, \\
\widetilde{\alpha}_{ij} &= \frac{\partial \widetilde{u}_j}{\partial x_i}.
\end{aligned} \tag{S4}$$

$\overline{\Delta}_m$ is the filter width in the m-direction and C_v is the model coefficient, which is set equal to 0.07 as proposed by Vreman (2004). Even with a non-zero model coefficient, zero Π, and therefore, zero eddy viscosity is obtained in laminar and fully resolved flows.

S1.2. Energy transport

The LES compressible flow equation in CONVERGE code for temperature can be written as:

$$\frac{\partial \overline{\rho} c_v \widetilde{T}}{\partial t} + \frac{\partial \overline{\rho} c_v \tilde{u}_j \widetilde{T}}{\partial x_j} = -\frac{\partial \tilde{u}_j \bar{p}}{\partial x_j} + \frac{\partial}{\partial x_j}(\widetilde{\sigma}_{ij}\tilde{u}_i + \tilde{k}\widetilde{T} - c_v q_j), \tag{S5}$$

where $\widetilde{T}_i$ is the temperature, c_v is the specific heat at constant volume, $\tilde{k}$ is thermal conductivity, and $q_j = \overline{\rho}(\widetilde{u_j T} - \tilde{u}_j \tilde{T})$ is the SGS heat flux. The SGS

heat flux is approximated as following:

$$q_j = -\frac{\nu_t}{Pr_t}\frac{\partial \widetilde{T}}{\partial x_j}. \tag{S6}$$

where Pr_t is the SGS Prandtl number which is assumed to be 0.7.

S1.3. Species transport

The LES compressible flow equations in CONVERGE code for transport of species mass fractions become:

$$\frac{\partial \overline{\rho}\widetilde{Y_i}}{\partial t} + \frac{\partial \overline{\rho}\tilde{u}_j\widetilde{Y_i}}{\partial x_j} = \frac{\partial}{\partial x_j}(\widetilde{\lambda}_j^i - T_j^i) + \overline{\dot{\omega}}_i, \tag{S7}$$

where $\widetilde{Y_i}$ is the species mass fraction, $\widetilde{\lambda}_j^i$ is the diffusive flux, $T_j^i = \overline{\rho}(\widetilde{u_j Y_i} - \tilde{u}_j\widetilde{Y_i})$ is the SGS flux, and $\overline{\dot{\omega}}_i$ is the production rate of species i. The SGS flux is approximated using gradient-diffusion approximation as following:

$$T_j^i = -\frac{\nu_t}{Sc_t}\frac{\partial \widetilde{Y_i}}{\partial x_j}. \tag{S8}$$

where Sc_t is the SGS Schmidt number which is assumed to be 0.7. The filtered species production rate, $\overline{\dot{\omega}}_i$, is calculated using the filtered quantities without accounting for the effect of SGS fluctuations.

S1.4. Aerosol particle transport

Transport and microphysics of aerosol particles is governed by the general dynamic equation (GDE). The GDE describes particle evolution due to convection, diffusion, condensation/evaporation, coagulation, and nucleation etc. The GDE is written in discrete form as a population balance on each cluster/particle size. Direct solution of GDE is computationally unfeasible. Therefore, GDE is discretized in particle number and mass space, where the entire particle distribution is divided into discrete number of bins, B. The equation is then solved as set of B transport equations. The LES transport equation for the number concentration of particles, $\widetilde{N}_k$ in bin k, is given by

$$\frac{\partial \overline{\rho}\widetilde{N}_k}{\partial t} + \frac{\partial \overline{\rho}\tilde{u}_j\widetilde{N}_k}{\partial x_j} = \frac{\partial}{\partial x_j}(\widetilde{\lambda}_j^k - Q_j^k) + \overline{\dot{\omega}_k^N}, \tag{S9}$$

where $\widetilde{N}_k$ is the aerosol number concentration, $\widetilde{\lambda}_j^k$ is the diffusion flux, $Q_j^k = \overline{\rho}(\widetilde{u_j N_k} - \tilde{u}_j \widetilde{N}_k)$ is the SGS flux, and $\overline{\dot{\omega}_k^N}$ is the source term due to aerosol microphysics for bin k. The SGS flux is approximated using gradient-diffusion approximation as following:

$$Q_j^i = -\frac{\nu_t}{Sc_t}\frac{\partial \widetilde{N}_k}{\partial x_j}, \tag{S10}$$

where Sc_t is SGS Schmidt number which is assumed to be 0.7. In calculation of the diffusion flux, $\widetilde{\lambda}_j^k$, particle diffusivity, D_k, is calculated as following:

$$D_k = k_b \widetilde{T}\frac{C_c}{3\pi\mu d_{p_k}}. \tag{S11}$$

where k_b is the Boltzmann constant, C_c is the Cunningham correction factor, and d_{p_k} is the particle diameter for bin, k. The filtered source term, $\overline{\dot{\omega}_k^N}$, is closed by assuming that the aerosol microphysics depends only the filtered quantities. In other words, it is assumed that $\overline{\dot{\omega}_k^N} = \dot{\omega}_k^{\overline{N}}$, or that $\dot{\omega}_k^{SGS} = 0$. Loeffler et al. (2011) performed simulations of nanoparticle formation and growth in a turbulent jet under the same assumption and found that LES predictions agreed reasonably well with the fully-resolved direct numerical simulation (DNS) results. Garmory & Mastorakos (2008) performed simulations of aerosol nucleation and growth in a turbulent jet using stochastic fields method that accounts for effect of turbulent fluctuations on nucleation and growth. They found that the width of the nucleation zone predicted with the stochastic fields method was slightly larger as compared to when the effect of turbulent fluctuations was ignored. However, the authors concluded that the predictions of the total number concentration is dependent more on thermodynamic properties and empirical correlations used, rather than the incorporation of turbulent fluctuations into the aerosol dynamics equations.

The above described approach for transport of particles assumes that particles follow the flow, and that the motion of particles does not affect the flow field. The particles will deviate from flow lines for three reasons: 1) very small particles due to diffusion (included here), 2) very large particles for gravitational settling (not included but negligible for the size range of particles in exhaust emissions), and 3) thermophoresis (not included but negligible for temperature gradient in the tunnel). This assumption is quite reasonable for sub-micron size particles considered in this work (Lipsky &

Robinson, 2005). Aerosol microphysics is incorporated into the CONVERGE code using user defined functions (UDFs).

S1.5. Computational grid

An octree meshing strategy was used in CONVERGE for local grid refinement. The computational grid was guaranteed to conform to the geometry by allowing polyhedral cell shapes near the boundary. Therefore, while bulk of the computational domain was composed of perfectly orthogonal hexahedral grid cells, polyhedral cells of arbitrary shape existed near the boundaries. For reference, computational grid for the cross-flow tunnel is shown in Fig. S1. Only a portion of the grid on a two dimensional plane is shown in Fig. S1. Local grid-refinement is used to allow larger number of cells in regions where the sample and dilution air mix. The grid is gradually coarsened away from the sample inlet to obtain a lower total number of cells. Near the inlet of the sample, the cell size is approximately 1.16 mm for both tunnels. As discussed in the next Section, this cell size was achieved based on a grid sensitivity analysis. For the grid shown in Fig. S1, an approximate total numbers of cells in the cross-flow tunnel are 4×10^5. Same resolution for the axial-flow tunnel results in 3.2×10^5 total cells.

S2. Grid sensitivity analysis and time averaging

Grid sensitivity analysis is performed for the cross-flow tunnel using 2×10^5 (200k), 3×10^5 (300k), and 4×10^5 (400k) grid cells in the entire computational domain. The computational cell size is 1.5 mm, 1.3 mm, and 1.16 mm near the sample exit for the 200k, 300k, and 400k grids, respectively. The predictions of dilution-corrected (cm^{-3} of exhaust sample) total particle number concentration (N) at the tunnel exit are shown in Fig. S2 for DR 20 and 110. It is common for purely theoretical nucleation parameterizations to predict nucleation rates that are incorrect by several orders of magnitude. Therefore, a correction factor was applied, and the binary nucleation rate was multiplied by 35 for the 200k grid, and by 25 for the 300k and 400k grids to match the experimentally measured total N for DR of 20. The DR 20 case was chosen for tuning of the nucleation rate because of larger number of nucleation-mode particles observed in the experiments. As shown in Fig. S2, the predicted total N, and the trend between the two dilution ratios, are both sensitive to the grid. For the 200k grid, the predicted total N is higher for DR 110, while for the 300k and 400k grids, the predicted total N is higher

for DR 20. As discussed in the next Section, the predicted trend agrees better with the experimental measurements for the 300k and 400k grids. Since the predicted trend did not change significantly from 300k to 400k grids, the grid with 400k cells is used for rest of the simulations of the cross-flow tunnel. For the axial-flow tunnel, the cells size near the sample exit is the same as for the cross-flow tunnel, but due to a smaller size of the tunnel, the total number of cells is about 320k. For all simulations discussed in the main document, the nucleation rate is multiplied by a factor of 25. For all cases, timestep for simulations was chosen based on Courant-Friedrichs-Lewy (CFL) condition. CFL number for both convection and diffusion were set to 1.0. The flow field and aerosol distribution in the tunnel were allowed to develop for one flow through time before collecting statistics. Data presented in Figure 5, Figure 6, Figure 9(b), and Figure 9(d) of the main document were then obtained by averaging for one flow through time.

References

Garmory, A., & Mastorakos, E. (2008). Aerosol nucleation and growth in a turbulent jet using the stochastic fields method. *Chemical Engineering Science*, *63*, 4078–4089.

Lipsky, E. M., & Robinson, A. L. (2005). Design and evaluation of a portable dilution sampling system for measuring fine particle emissions from combustion systems. *Journal of Aerosol Science and Technology*, *39*, 542–553.

Loeffler, J., Das, S., & Garrick, S. C. (2011). Large eddy simulation of titanium dioxide nanoparticle formation and growth in turbulent jets. *Journal of Aerosol Science and Technology*, *45*, 616–628.

Vreman, A. W. (2004). An eddy-viscosity subgrid-scale model for turbulent shear flow: algebraic theory and applications. *Physics of Fluids*, *16*, 3670–3681.

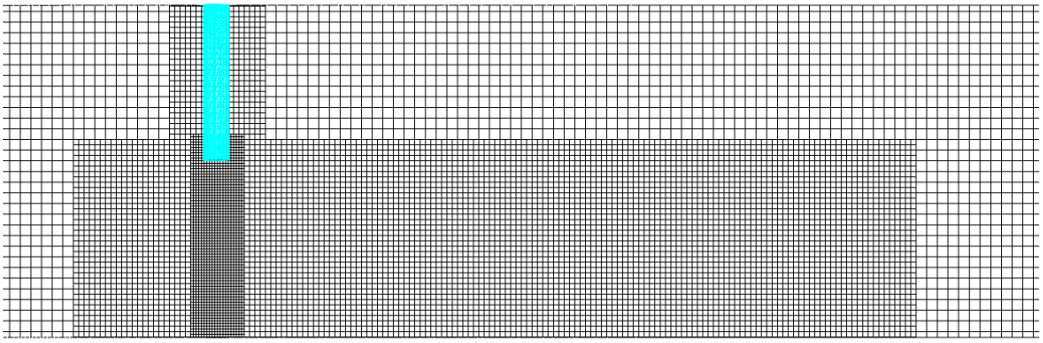

(a)

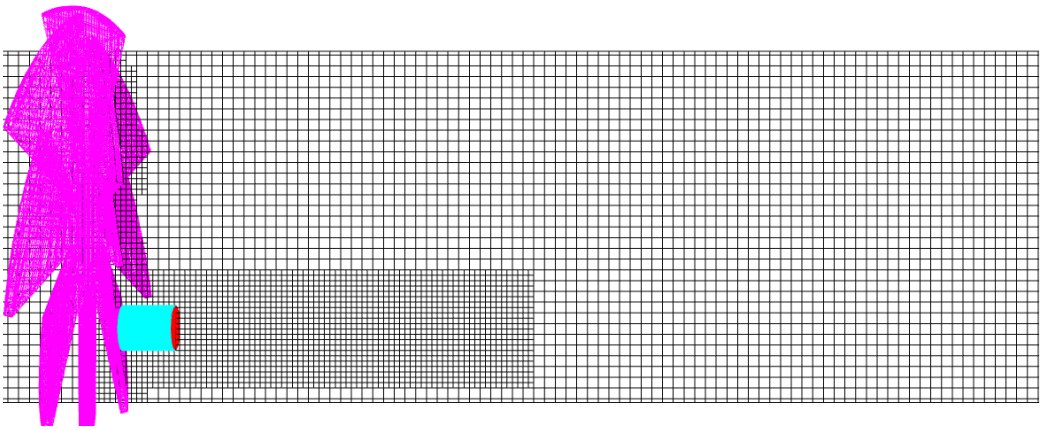

(b)

Figure S1: Computational grid for (a) the cross-flow tunnel with 4×10^5 (b) the axial-flow tunnel with 3.2×10^5 total cells in the entire tunnel. Only regions of the tunnels near the sample inlet are shown. For reference, the diameters of the cross-flow and axial-flow tunnels are 0.15 m and 0.11 m, respectively.

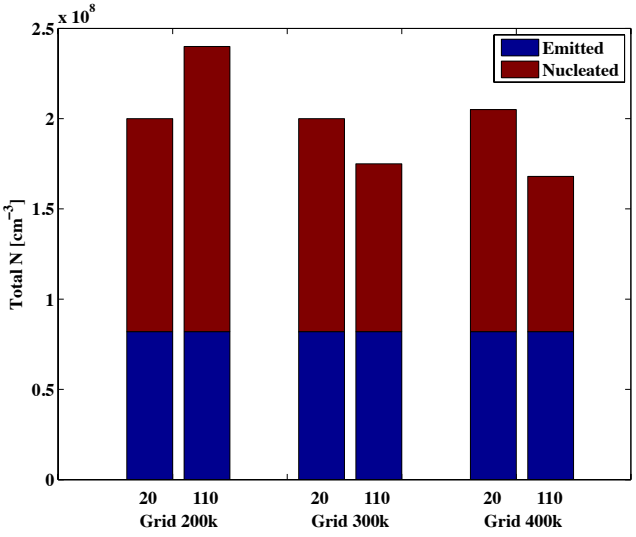

Figure S2: Predictions of total N at the tunnel exit for three different grids for the cross-flow (CF) tunnel at DR = 20 and 110.